Tyrosyl Interactions in the Folding and Unfolding of Bovine Pancreatic Ribonuclease A: A Study of Tyrosine-to-Phenylalanine Mutants†

D. Juminaga, W. J. Wedemeyer, R. Garduño-Júarez,‡ M. A. McDonald, and H. A. Scheraga*

Baker Laboratory of Chemistry, Cornell University, Ithaca, New York 14853-1301

Received March 26, 1997; Revised Manuscript Received June 12, 1997⊗

ABSTRACT: Three tyrosine-to-phenylalanine mutants of ribonuclease A (Y25F, Y92F, and Y97F) are investigated for their enzymatic activities, molecular stabilities, and unfolding/refolding kinetics. These mutants exhibit 80, 90, and 80%, respectively, of the catalytic activity of the wild-type enzyme. Thermal, Gdn·HCl, and pH transition measurements indicate that Y25F and Y97F are less stable than the wild-type protein, whereas the bulk of the thermodynamic and kinetic evidence indicates that Y92F is as stable as the wild-type protein. Differences in molar extinction coefficients indicate that tyrosines 25, 92, and 97 contribute 38, 13, and 39%, respectively, to the absorption difference between the folded and unfolded states, in general agreement with previous studies but possibly indicating the contribution of a fourth tyrosine residue to account for the remaining 10%. Stopped-flow single- and double-jump kinetic experiments were carried out on the wild-type and three mutant proteins. At least one tyrosine residue besides tyrosine 92 contributes to the slow fluorescence-unfolding phase; the likely candidate for this residue is tyrosine 115 which monitors the cis−trans isomerization of the X−Pro114 peptide bond. Tyrosines 25 and 97 are involved in interactions that retard conformational unfolding and accelerate conformational refolding as well as the cis−trans proline isomerization of the slow-refolding phases, presumably by stabilizing the major β-hairpin structure of RNase A. These interactions may contribute to the strong pH dependence of the folding and unfolding of ribonuclease A. In contrast, tyrosine 92 does not affect the folding and unfolding rates significantly. An improved "box" model of proline isomerization under unfolding conditions was derived from exhaustive fitting of all possible box models. The kinetic data support the identification of Pro93 as the proline whose isomerization distinguishes the slow-*refolding* species (U_S^{II} and U_S^{I}) from the other, faster-refolding species (U_{vf}, U_f, and U_m), implying that Pro93 isomerizes in the slow-refolding reactions $U_S^{I} \rightarrow N$ and $I_N \rightarrow N$. Similarly, Pro114 seems to distinguish between the very fast-refolding species U_{vf} and the fast-refolding species U_f. Lastly, Pro117 seems to distinguish the major slow-refolding species U_S^{II} from the minor slow-refolding species U_S^{I} and the medium-refolding species U_m from the fast- and very fast-refolding species.

An important aspect of the protein folding problem is the determination of the specific interactions that influence the folding pathways and lead to the structure of the folded species. In this study, the role of tyrosyl interactions in the folding/unfolding of disulfide-intact ribonuclease A is investigated using site-specific mutagenesis.

Physicochemical experiments indicated that three tyrosines of RNase A[1] (residues 25, 92, and 97; Figure 1) are buried in the native state and titrate abnormally ($pK_a > 11.5$), although tyrosine 92 seems only partially buried; further experiments suggested that the hydroxyl groups of these tyrosines interact with nearby abnormally titrating aspartates, residues 14, 38, and 83, respectively (Scheraga, 1957, 1967, 1984). X-ray and NMR studies have largely confirmed this model, although, in addition, the hydroxyl groups of tyrosines 92 and 97 seem to be hydrogen bonded to the carbonyl oxygen of lysines 37 and 41, respectively (Wlodawer et al., 1988; Baker & Kintanar, 1996; Eberhardt et al., 1996).

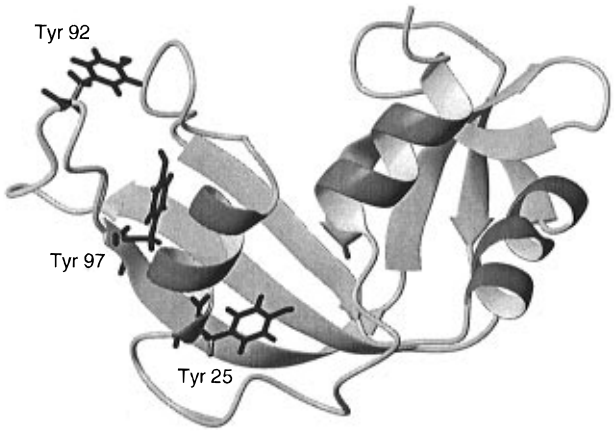

FIGURE 1: Ribbon diagram of ribonuclease A with the mutated tyrosines indicated. The structure was taken from Wlodawer et al. (1988). The diagram was prepared with the program MOLMOL (Koradi et al., 1996).

† This work was supported by Grant GM-24893 from the National Institute of General Medical Sciences of the National Institutes of Health. Support was also received from the National Foundation for Cancer Research. W.J.W. was a NIH Trainee (1993−1996). R.G.J. thanks CONACYT-México (Consejo Nacional de Ciencía y Tecnologia de México) and DGAPA-UNAM (Dirección General de Asuntos del Personal Académico, Universidad Nacional Autónoma de México) for sabbatical fellowships during his stay at Cornell University.

* Author to whom correspondence should be addressed.

‡ On leave from the Instituto de Física, Universidad Nacional Autónoma de México, Lab. de Cuernavaca, Apdo. Postal 48-3, 62251 Cuernavaca, Morelos, México.

⊗ Abstract published in *Advance ACS Abstracts,* August 1, 1997.

[1] Abbreviations: RNase A, bovine pancreatic ribonuclease A; cCMP, cytidine 2′,3′-cyclic monophosphate; Gdn·HCl, guanidine hydrochloride; Gdn·SCN, guanidine thiocyanate; NTB, 2-nitro-5-thiobenzoate; NTSB, disodium 2-nitro-5-thiosulfobenzoate.

S0006-2960(97)00711-3 CCC: $14.00

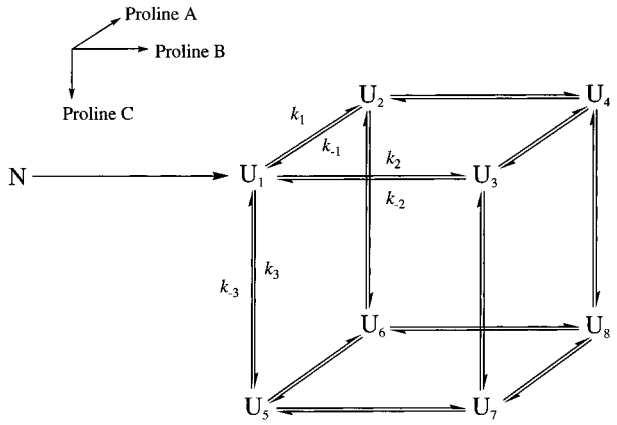

FIGURE 2: Generic box unfolding model of ribonuclease A from the native conformation (N) to various unfolded species (U_1-U_8). It is assumed that the three directions of the box correspond to three independent proline isomerizations (Houry et al., 1994; Dodge & Scheraga, 1996; Houry & Scheraga, 1996a), designated initially in terms of prolines A, B, and C.

These three tyrosine residues are also responsible for the UV difference spectra between the folded and unfolded protein (Woody et al., 1966). Consequently, the folding kinetics of disulfide-intact ribonuclease A have been followed by stopped-flow experiments based on the absorption and fluorescence of these tyrosine residues (Tsong et al., 1972; Garel & Baldwin, 1973, 1975; Garel et al., 1976; Houry et al., 1994; Houry & Scheraga, 1996a). Multiple refolding phases have been observed under various conditions; the heterogeneity in the unfolded state arises, at least partly, from the cis−trans isomerization of X−Pro peptide bonds (Brandts et al., 1975; Cook et al., 1979; Schmid, 1982; Schmid et al., 1986). In the folded state of RNase A, two of the X−Pro peptide bonds (Tyr92−Pro93 and Asn113−Pro114) are in the cis conformation, while the other two (Lys41−Pro42 and Val116−Pro117) are in the trans conformation (Wlodawer & Sjölin, 1983; Wlodawer et al., 1988). During unfolding, all four X−Pro peptide bonds isomerize and achieve an equilibrium between roughly 30 cis and 70% trans conformations. This partitioning of the X−Pro peptide bonds into two distinct conformations contributes to the heterogeneity of the unfolded state (Rehage & Schmid, 1982; Lin & Brandts, 1983; Adler & Scheraga, 1990; Schultz et al., 1992; Houry & Scheraga, 1996a). Because of the large activation energy (∼20 kcal/mol), the isomerization between the trans and cis conformations is a slow process and can be the rate-limiting step in folding (Brandts et al., 1975).

Using double-jump techniques and proline-to-alanine mutants, three prolines were shown to be essential to the heterogeneous kinetics of ribonuclease A, namely Pro93, Pro114, and Pro117 (Dodge et al., 1994; Dodge & Scheraga, 1996). The cis−trans isomerizations of these X−Pro peptide bonds under unfolding conditions give rise to eight unfolded species, arranged in a generic "box" model (Figure 2). A specific box model has been proposed which associates these eight unfolded species with the five observed refolding phases (Houry et al., 1994; Dodge & Scheraga, 1996; Houry & Scheraga, 1996a). In this model, native RNase A unfolds rapidly to form a very fast-refolding species (U_{vf}; U_1 in Figure 2) that retains the native X−Pro peptide bond conformations, followed by cis−trans isomerization of X−Pro peptide bonds to form other unfolded species, e.g. U_f, U_m, U_S^{II}, and U_S^{I} corresponding to the fast-, medium-, major slow-, and minor slow-refolding phases.

The refolding of some unfolded species has been studied in detail. The refolding of U_{vf} is a very fast process driven by hydrophobic collapse to form a partially folded "molten-globule" intermediate (I_Φ) (Houry et al., 1995; Houry & Scheraga, 1996b). The refolding of U_S^{II} involves a hydrogen-bonded intermediate (I_1), which subsequently forms a native-like intermediate (I_N); the refolding from I_N to the native structure (N) is rate-limited by the cis−trans isomerization of at least one X−Pro peptide bond (Cook et al., 1979; Schmid & Baldwin, 1979; Kim & Baldwin, 1980; Schmid & Blaschek, 1984; Udgaonkar & Baldwin, 1988, 1990, 1995).

In the present study, the significance of the three buried tyrosines and their interactions with nearby residues, in particular the nearby aspartate groups, for the folding pathway of disulfide-intact ribonuclease A is investigated using three tyrosine-to-phenylalanine mutants (Y25F, Y92F, and Y97F). The effects of these mutations on the enzymatic activity and molecular stability are determined from the rate of hydrolysis of cCMP and from pH, thermal, and Gdn·HCl transitions, respectively, while the effects on the folding pathway are investigated by stopped-flow kinetic experiments.

Our results indicate that tyrosines 25 and 97 are completely buried in the native structure of wild-type RNase A, whereas tyrosine 92 is partially buried; another partially buried tyrosine cannot be ruled out, however. Furthermore, tyrosine 92 is not solely responsible for the slow fluorescence-unfolding phase; our experiments and kinetic fits indicate that tyrosine 115 may also contribute since its fluorescence properties may monitor the cis−trans isomerization of the X−Pro114 peptide bond. The kinetic studies indicate that tyrosines 25 and 97 are involved in interactions that decelerate conformational unfolding and accelerate conformational folding, as well as the cis−trans isomerization observed in the slow-refolding phases, in wild-type RNase A. The data also suggest that tyrosines 25 and 97 may contribute to the pH dependence of the folding and unfolding of RNase A. Fits of double-jump experiments to all possible box models indicate that the Y92F mutation does not significantly influence the rates of proline isomerization under unfolding conditions. Furthermore, the isomerization properties of the three essential prolines of RNase A were investigated; an assignment of these prolines to an improved box model is proposed.

MATERIALS AND METHODS

Purification of Wild-Type Ribonuclease A. Wild-type bovine pancreatic ribonuclease A type 1-A (Sigma) was purified by cation exchange chromatography according to the procedure of Rothwarf and Scheraga (1993).

Expression and Purification of the Tyrosine-to-Phenylalanine Mutants. Site-directed mutageneses were carried out

[2] Y25F, Y92F, and Y97F are the tyrosine-to-phenylalanine mutants of RNase A, corresponding to tyrosines 25, 92, and 97, respectively. U_{vf}, U_f, U_m, U_S^{I}, and U_S^{II} are ensembles of unfolded species corresponding to the very fast-, fast-, medium-, minor slow-, and major slow-refolding phases, respectively. α_{vf}, α_f, α_m, α_{SI}, and α_{SII} and τ_{vf}, τ_f, τ_m, τ_{SI}, and τ_{SII} are the corresponding amplitudes and time constants, respectively, for the folding kinetics of each of these phases.

[3] RNase A refers to *disulfide-intact* bovine pancreatic ribonuclease A; the wild-type protein corresponds to the natural (not recombinant) RNase A.

using the T7-Gen *in vitro* mutagenesis kit (United States Biochemical) on a synthetic gene for bovine pancreatic ribonuclease A, a gift from the Genex Corp., and the products were placed in the M13mp18 vector (United States Biochemical) according to the procedure of Laity et al. (1993). The synthetic oligonucleotides used for the site-directed mutageneses were synthesized at the Cornell Biotechnology Analytical Facility. Y25F, Y92F, and Y97F genes were created by changing the codons of tyrosines 25, 92, and 97, respectively, to TTT (phenylalanine). Originally, the mutant genes were incorporated in the pSJIIGEM-2 vector to be expressed as gene 10 fusion proteins in *Escherichia coli* strain HMS174(DE3)-pLys(S) (Novagen) using procedures described by Laity et al. (1993). Later, the mutant genes were transferred to the pET22b(+) vector (Novagen) and expressed in *E. coli* strain BL21(DE3) (Novagen) to obtain better expression yields (delCardayré et al., 1995). *Msc*I sites were created upstream starting at the 5′-end of the mutant genes in the pSJIIGEM-2 vectors, and the mutant genes were cloned into the pET22b(+) vectors between the *Msc*I and *Hind*III restriction enzyme sites. The procedures for the expression and purification of the mutant proteins are described by Dodge and Scheraga (1996). The correctness of the mutations was confirmed by DNA sequencing, amino acid analysis, and peptide mapping.

Determination of the Extinction Coefficient. All of the absorption measurements in this study were carried out with a modified Cary model 14 spectrophotometer (Denton et al., 1982). The molar extinction coefficients of the wild-type and mutant proteins were determined by means of an NTSB assay for disulfides (Thannhauser et al., 1987). The absorbances of approximately 1 mg/mL of the protein stock solutions (in 100 mM acetic acid) were measured at 275 nm. The NTSB assay was carried out by mixing 60 μL of the protein stock solution with 1220 μL of the assay buffer (2 M Gdn·SCN, 50 mM glycine, 300 mM sodium sulfite, 3 mM EDTA, and 25 mM NTSB at pH 9.5). The formation of NTB was followed by measuring the absorption at 412 nm, and the concentration of NTB formed was determined using 13 900 M^{-1} cm^{-1} as the molar extinction coefficient of NTB at 412 nm (Thannhauser et al., 1987). The resulting concentration of NTB was then used to calculate the concentration of the protein stock solution and, hence, the molar extinction coefficients of the proteins at 275 nm.

Differences in extinction coefficients at 287 nm ($\Delta\epsilon_{287}$) between the folded and unfolded protein were determined at room temperature. The folded protein was prepared in 0.6 M Gdn·HCl and 0.1 M sodium acetate at pH 5.0, while the unfolded protein was prepared by diluting the folded protein 2.5-fold with 5.6 M Gdn·HCl and 120 mM glycine at pH 2.0 so that the final condition was 4.2 M Gdn·HCl at pH 2.0.

Determination of Enzymatic Activities. The enzymatic activities were determined from the catalytic rate of hydrolysis of cytidine 2′,3′-cyclic monophosphate (cCMP) (Sigma) at 25 °C in 100 mM acetic acid at pH 5 (Crook et al., 1960). The rates of catalysis were monitored by absorption at 287 nm, and the slopes (Δabsorbance/Δtime) divided by concentrations of the wild-type protein and the mutants were compared. The relative rates of catalysis are reported as percentages of the wild-type rate.

Thermal Denaturation. The concentration of the protein solution used in the measurements was 1 mg/mL; the buffer used was 10 mM sodium acetate at pH 4.0. The change in absorption at 287 nm as a function of temperature was measured with a modified Cary model 14 spectrophotometer (Denton et al., 1982). A calibrated thermistor was used to record the temperature of the sample compartment which was maintained by a Neslab RTE-100 circulation bath. The circulation bath was interfaced to a SUN IPC computer which contained a program to control the temperature of the water bath so that the temperature was raised and lowered in a stepwise manner allowing 20 min for equilibration at each temperature below 50 °C, 15 min between 50 and 60 °C, and 10 min above 60 °C.

The transitions were analyzed by fitting the primary absorption data as described by Santoro and Bolen (1988). The difference in free energy ΔG between the folded and unfolded states was assumed to follow the functional form

$$\Delta G = \Delta H_m(1 - T/T_m) - \Delta C_p[(T_m - T) + T\ln(T/T_m)]$$

as described by eq 37 of Privalov (1979), where ΔH_m is the difference in enthalpy at the transition temperature T_m and the difference in heat capacity ΔC_p was fixed at its calorimetric value (Makhatadze & Privalov, 1995). The pre- and post-transitional regions were fit by straight lines as in Santoro and Bolen (1988). The 95% confidence limits were determined from 1000 Monte Carlo runs according to the method described in Press et al. (1992).

Guanidine Hydrochloride Transitions. A series of protein solutions (1 mg/mL), dissolved in 0.1 M sodium acetate at pH 5.0 at various concentrations of Gdn·HCl, was allowed to equilibrate at 15 °C overnight. Gdn·HCl concentrations were determined by measuring refractive indices of the solutions at 25 °C (Nozaki, 1972) using a Bausch and Lomb refractometer. The absorbance at 287 nm was measured with a modified Cary model 14 spectrophotometer (Denton et al., 1982) with the sample compartments maintained at 15 °C. The transitions were analyzed by fitting the primary data as described by Santoro and Bolen (1988) with the added assumption that the pre- and post-transition slopes are zero. Owing to the large uncertainties in the fitted *m* values, the tabulated values of $\Delta\Delta G°$ were determined directly from the transition midpoints while fixing *m* at 3.0 kcal mol^{-1} M^{-1} (Pace et al., 1989). The 95% confidence limits were determined from 1000 Monte Carlo runs according to the method described in Press et al. (1992).

pH Transitions. A series of protein solutions was prepared by diluting (1:20) the protein stock solution with buffers with different pH's. For pH 1.0−3.0, the buffer used was 0.2 M glycine, while for pH 3.2−4.2, the buffer used was 0.2 M sodium acetate. The final concentration of the wild-type and Y97F protein solutions was ∼0.8 mg/mL, while that of the Y25F and Y92F protein solutions was ∼0.5 mg/mL. The pH's of the wild-type protein solutions were remeasured, and it was found that the dilutions did not alter the buffer pH significantly. The absorbances at 287 nm of these protein solutions were measured at 22 and 37 °C with a modified Cary 14 spectrophotometer (Denton et al., 1982); the temperature was maintained by a Neslab RTE-100 circulation bath, and the samples were pre-equilibrated at this temperature overnight before measurements. The midpoints of transitions were determined by the method described by Pace et al. (1989). The difference in proton binding ($\Delta\nu$) between the folded and unfolded states was estimated by fitting the

pH transition data to eq 1 of Hermans and Scheraga (1961b), which is equivalent to

$$\partial(\ln K_{eq})/\partial(\mathrm{pH}) = 2.303\Delta\nu$$

where the effective equilibrium constant K_{eq} (between the folded and unfolded forms) was evaluated as in Hermans and Scheraga (1961b).

Stopped-Flow Kinetic Experiments. The experimental setup, using a Hi-Tech PQ/SF-53 stopped-flow apparatus, has been described by Houry et al. (1994). The flow cell had a path length of 10 mm and a width of 2 mm. All measurements were carried out at 15 °C. For absorption measurements, a deuterium lamp (Hellma) was used as a light source, and the monochromator for the incident light was set at 287 nm. For fluorescence measurements, a xenon arc lamp (Ushio, Japan) was used; the excitation wavelength was set at 268 nm, and a band-pass filter (280−400 nm) was used for emission. Data were collected every 0.5 ms for the first minute and every 50 ms thereafter, for up to 20 min.

Three types of experiments were carried out, including single-jump unfolding, single-jump refolding, and double-jump refolding; the latter was used to track the refolding amplitudes as a function of unfolding time (Houry et al., 1994). For single-jump unfolding, 20 μL of protein solution (1.9 mg/mL) in 1.2 M Gdn·HCl and 50 mM sodium acetate at pH 5.0 was mixed with 100 μL of unfolding buffer, 4.8 M Gdn·HCl, and 50 mM glycine at pH 1.6 so that the final condition was 4.2 M Gdn·HCl at pH 2.0. For measurement of the activation energy for Y92F, this procedure was repeated at different temperatures.

For single-jump refolding, 11 μL of protein solution (13 mg/mL, except for Y97F which was 11 mg/mL) in 4.2 M Gdn·HCl and 40 mM glycine at pH 2.0 was mixed with 110 μL of refolding buffer, 0.2 M Gdn·HCl,and 50 mM sodium acetate at pH 5.3 so that the final condition was 0.6 M Gdn·HCl at pH 5.0.

For double-jump refolding in 0.9 M Gdn·HCl at pH 5.0, the protein was first unfolded in 4.2 M Gdn·HCl at pH 2.0 by mixing 52 μL of protein solution (21 mg/mL) in 0.6 M Gdn·HCl and 100 mM sodium acetate at pH 5.0 with 130 μL of unfolding buffer, 5.6 M Gdn·HCl, and 120 mM glycine at pH 0.9 for unfolding times ranging from 0.5 to 600 s. Then the protein was refolded in 0.9 M Gdn·HCl at pH 5.0 by mixing 70 μL of the unfolded protein solution with 350 μL of refolding buffer, 0.2 M Gdn·HCl, and 100 mM sodium acetate at pH 5.5. For double-jump refolding in 1.3 M Gdn·HCl at pH 5.0, the protein was first unfolded in 4.0 M Gdn·HCl at pH 2.0 by mixing 52 μL of protein solution (21 mg/mL) in 1.3 M Gdn·HCl and 40 mM sodium acetate at pH 5.0 with 130 μL of unfolding buffer, 5.1 M Gdn·HCl, and 40 mM glycine at pH 2.0 for unfolding times ranging from 0.5 to 600 s. Then the protein was refolded in 1.3 M Gdn·HCl at pH 5.0 by mixing 70 μL of the unfolded protein solution with 350 μL of refolding buffer, 0.8 M Gdn·HCl, and 100 mM sodium acetate at pH 5.2.

Data obtained from all stopped-flow measurements were fit to a sum of exponentials with the program PLOT from New Unit (Ithaca, NY), using a Levenberg−Marquardt algorithm (Marquardt, 1963) for nonlinear least-squares fitting. The variances of the amplitudes and time constants were calculated using the formula $(n-1)^{-1}\Sigma(y-\bar{y})^2$, where

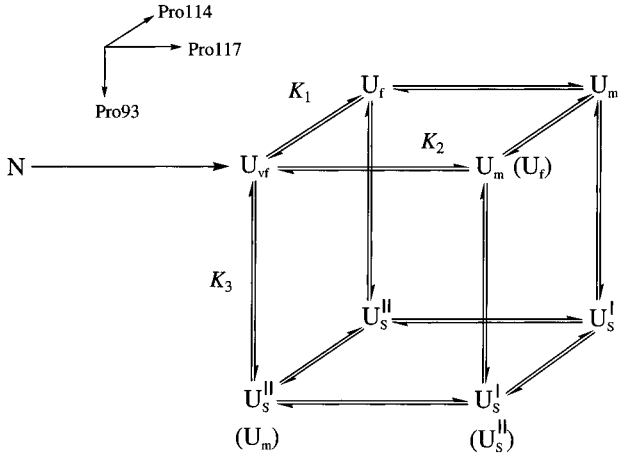

FIGURE 3: Best-fitting box model of RNase A under unfolding conditions derived from the double-jump experiments of this study. K_1, K_2, and K_3 are the equilibrium constants for the three directions of the box. The assignments of the previous box model (Dodge & Scheraga, 1996; Houry & Scheraga, 1996a) that differ from those of the new box model are indicated in parentheses.

y is the fitted value of the amplitude or time constant, $\bar{y}$ is the average value, and n is the number of runs. All errors are listed at the 95% confidence limit.

Exhaustive Fitting. The double-jump data were fit exhaustively to box models representing the isomerization of the three essential prolines of RNase A (Figure 2). A specific box model is defined by associating its eight species with the experimentally observed refolding phases (U_{vf}, U_f, U_m, U_S^{II}, and U_S^{I}). The relative amplitude of each refolding phase is assumed to be equal to the sum of the relative concentrations of its associated species when refolding is initiated (Houry et al., 1994). As an example, consider the specific box model of Figure 3, in comparison with the generic model of Figure 2. The relative refolding amplitudes are given by

$$\%\alpha_{vf} = [U_1]$$

$$\%\alpha_f = [U_2]$$

$$\%\alpha_m = [U_3] + [U_4]$$

$$\%\alpha_S^{II} = [U_5] + [U_6]$$

$$\%\alpha_S^{I} = [U_7] + [U_8]$$

where $[U_k]$ represents the relative concentrations of the various unfolded species. For example, the relative refolding amplitude of U_S^{II} should be equal to the combined relative concentrations of U_5 and U_6 at the moment when refolding is initiated.

The double-jump data were fit to all such box models (i.e. to all possible pairings of U_1−U_8 with the refolding phases) meeting two criteria. The first criterion was that the rate constants along the respective parallel edges of the box be equal, yielding three pairs of rate constants: k_1 and k_{-1}, k_2 and k_{-2}, and k_3 and k_{-3} (Figure 2). These rate constants correspond to the independent isomerizations of three prolines, denoted in Figure 2 as prolines A, B, and C, respectively. By assumption, these prolines correspond to the essential prolines in RNase A, Pro93, Pro114, and Pro117 (Dodge & Scheraga, 1996), although the assignment of the latter to the former is yet to be determined. (A tentative

Table 1: Summary of the Molecular Properties and Enzymatic Activities of Wild-Type RNase A and the Tyrosine-to-Phenylalanine Mutants

	ϵ_{275}[a]	$\Delta\epsilon_{287}$[b]	T_m (°C)[c]	$[Gdn{\cdot}HCl]_{1/2}$[d]	$pH_{1/2}$[e]	% activity[f]
wild type	9609 ± 117	2749 ± 127 (100%)	52.6 ± 0.2	2.99 ± 0.04	2.65	100
Y25F	8346 ± 149	1709 ± 75 (62 ± 6%)	46.1 ± 0.4	2.38 ± 0.02	3.20	80
Y92F	8407 ± 144	2382 ± 107 (87 ± 6%)	54.4 ± 0.4	3.03 ± 0.02	2.44	90
Y97F	8143 ± 72	1678 ± 95 (61 ± 7%)	47.7 ± 0.6	2.07 ± 0.02	3.18	80

[a] Molar extinction coefficients (M^{-1} cm^{-1}) at 275 nm at room temperature in 100 mM acetic acid. [b] Differences in molar extinction coefficients (M^{-1} cm^{-1}) at 287 nm at room temperature between the folded and unfolded protein. The folded condition was 0.6 M Gdn·HCl at pH 5.0, and the unfolded condition was 4.2 M Gdn·HCl at pH 2.0. The percentage contributions of tyrosines 25, 92, and 97 to the absorbance at 287 nm are 38 ± 6, 13 ± 6, and 39 ± 7%, respectively. The missing 10% may indicate the contribution of a fourth tyrosine, but the statistical errors are too large to warrant this conclusion. [c] Midpoints for the thermal transitions in 10 mM sodium acetate at pH 4.0 (Figure 4) determined by the method of Santoro and Bolen (1988) assuming the functional form found in Privalov (1979) with ΔC_p fixed at its calorimetric value (Makhatadze & Privalov, 1995). [d] Midpoints for the Gdn·HCl transitions at 15 °C in 100 mM sodium acetate at pH 5.0 (Figure 5) determined by the method of Santoro and Bolen (1988) with the added assumption that the pre- and post-transition slopes are zero. [e] Midpoints for the pH transitions at 37 °C (Figure 6) determined by the method of Pace et al. (1989). The buffer conditions are described in Materials and Methods. [f] Relative rates for the hydrolysis of cCMP reported as the percent of the wild-type rate. The rates refer to the initial slopes of the plots of absorbance at 287 nm, corresponding to the production of the substrate, versus time, at 25 °C in 100 mM acetic acid at pH 5.0.

assignment of these prolines will be made in the Discussion on the basis of the results of the fittings.) The second criterion was that a species could not refold faster than any species closer to U_1 (i.e. U_{vf}), all of whose prolines are in their native isomeric state. For example, the species U_7 cannot refold faster than U_3 or U_5, although it may refold at the same rate; thus, the assignment of U_f to U_7 and U_S^{II} to U_3 would be excluded by this second criterion.

For every such box model, the χ^2 statistic was minimized by varying the six rate constants to obtain the best fit to the double-jump data. The minimization was carried out by a simulated annealing simplex method (Press et al., 1992) beginning from many random starts; the resulting rate constants were robust and reproducible. The box model presented in Figure 3 is generally the best-fitting model on the basis of its reduced χ^2. The standard deviations for the final set of rate constants were determined from 1000 Monte Carlo runs as described in Press et al. (1992). The fitting programs were written in this laboratory and run on the IBM SP2 supercomputer of the Cornell Theory Center.

RESULTS

Molar Extinction Coefficients. The molar extinction coefficients at 275 nm of the wild-type protein and the tyrosine-to-phenylalanine mutants are shown in Table 1. The values for the mutants are lower by approximately 1300−1500 M^{-1} cm^{-1} compared to that of the wild-type protein, consistent with the loss of a tyrosine residue in each mutant (Pace et al., 1995).

Differences in molar extinction coefficients at 287 nm ($\Delta\epsilon_{287}$) between the folded and unfolded proteins are also presented in Table 1. The contribution of each tyrosine to the difference spectrum of the wild-type protein can be estimated from the *difference* in the values of $\Delta\epsilon_{287}$ between the wild-type protein and the corresponding mutant. The contributions of tyrosines 25, 92, and 97 to the wild-type total of 2749 ± 127 M^{-1} cm^{-1} are 1040 ± 147 M^{-1} cm^{-1} (38 ± 6%), 367 ± 166 M^{-1} cm^{-1} (13 ± 6%), and 1071 ± 158 M^{-1} cm^{-1} (39 ± 7%), respectively. These values are consistent with those reported by Bigelow (1961) and Woody et al. (1966). The missing 10% may indicate the contribution of a fourth tyrosine, but the statistical errors are too large to warrant this conclusion (see the Discussion).

Enzymatic Activities. The relative rates of hydrolysis of cCMP at pH 5.0 by the tyrosine-to-phenylalanine mutants and the wild-type protein are listed in Table 1. These indicate that the mutants are capable of catalyzing the hydrolysis of this substrate at rates comparable to that of the wild-type protein (Table 1), suggesting that the overall structure of the catalytic site, which includes histidines 12 and 119 and lysine 41 (Wlodawer et al., 1983), is conserved in the mutants. The relative rate for Y97F is consistent with that of Eberhardt et al. (1996), whose value of k_{cat} for Y97F is approximately 70% of that of the wild-type protein.

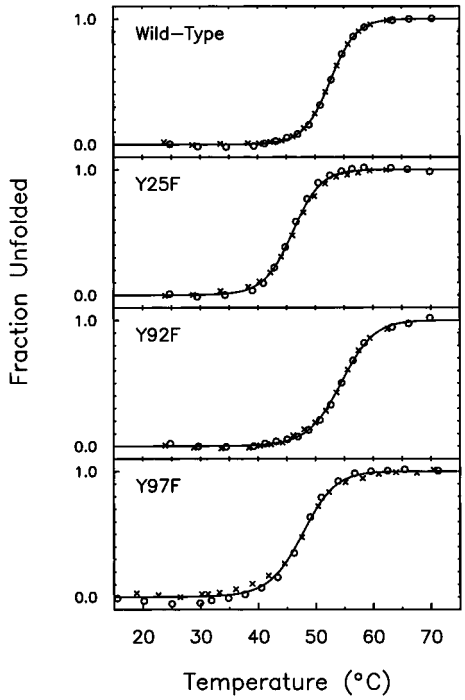

FIGURE 4: Thermal transition curves of the wild-type protein and the tyrosine-to-phenylalanine mutants of RNase A. The buffer conditions are 0.01 M sodium acetate at pH 4.0; ○ and × represent heating and cooling, respectively. The solid line is the fit to the free energy function described in the text. The parameters for the fit obtained by the method of Santoro and Bolen (1988) are listed in Tables 1 and 2. The fraction unfolded is calculated from the absorption difference at 287 nm.

Thermal and Gdn·HCl transitions of the wild-type and mutant proteins are shown in Figures 4 and 5, respectively. The heating and cooling curves for the thermal transition indicate that the unfolding of the wild-type and mutant proteins is reversible under the conditions used in this study. The thermodynamic parameters of the transitions, determined by the method of Santoro and Bolen (1988), are listed in Tables 1 and 2, along with their 95% confidence limits. These

Table 2: Thermodynamic Parameters for the Thermal and Gdn·HCl Transitions

	thermal transition[a]			Gdn·HCl transition[b]		pH transition[c]
	ΔH_m	ΔG (15 °C)	$\Delta\Delta G$ (15 °C)	m	$\Delta\Delta G°$ (15 °C)	$\Delta\nu$ (37 °C)
wild type	91.7 ± 5.0	7.72 ± 0.58	0	3.89 ± 0.70	0	2.1 ± 0.5
Y25F	82.0 ± 9.2	6.00 ± 0.92	1.72 ± 1.08	3.58 ± 0.48	1.83	1.2 ± 0.5
Y92F	73.9 ± 8.0	5.76 ± 0.96	1.96 ± 1.12	2.86 ± 0.28	−0.12	3.9 ± 1.0
Y97F	70.6 ± 11.2	5.01 ± 1.12	2.71 ± 1.26	3.50 ± 0.52	2.76	1.5 ± 0.5

[a] The parameters were obtained by the method of Santoro and Bolen (1988) assuming the functional form found in Privalov (1979) with ΔC_p fixed at its calorimetric value (Makhatadze & Privalov, 1995). ΔG and $\Delta\Delta G$ refer to a two-state equilibrium at pH 4.0 without denaturant (0 M Gdn·HCl). ΔH_m represents the difference in enthalpy at the transition temperature T_m. The units for ΔH_m, ΔG, and $\Delta\Delta G$ are kilocalories per mole. The error estimates refer to 95% confidence limits. [b] The parameters were obtained by the method of Santoro and Bolen (1988) with the added assumption that the pre- and post-transition slopes are zero. $\Delta\Delta G°$ was estimated from the transition concentrations ($[\text{Gdn·HCl}]_{1/2}$) by fixing m at 3.0 kcal mol^{-1} M^{-1} (Pace et al., 1989). $\Delta\Delta G°$ refers to a two-state equilibrium at 15 °C, pH 5.0, and 0 M Gdn·HCl. m represents the first derivative of the free energy difference with respect to the concentration of Gdn·HCl. The units of m and $\Delta\Delta G°$ are kilocalories per mole per molar and kilocalories per mole, respectively. The error estimates refer to 95% confidence limits. [c] The effective equilibrium constant was evaluated as in Hermans and Scheraga (1961b); the slope of the logarithm of the equilibrium constant versus pH was used to compute $\Delta\nu$, the difference in proton binding between the folded and unfolded states. The unit of $\Delta\nu$ is number of H^+ per protein molecule.

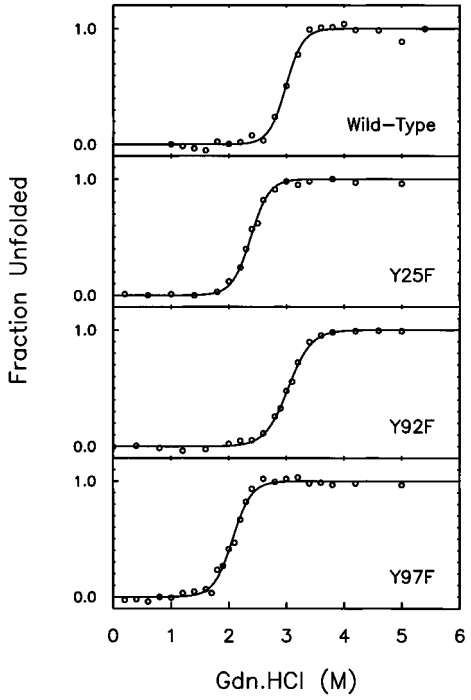

FIGURE 5: Gdn·HCl transition curves of the wild-type protein and the tyrosine-to-phenylalanine mutants of RNase A at 15 °C. The buffer conditions are 0.1 M sodium acetate at pH 5.0. The solid line is the fit to the free energy function described in the text. The parameters for the fit obtained by the method of Santoro and Bolen (1988) are listed in Tables 1 and 2. The fraction unfolded is calculated from the absorption difference at 287 nm.

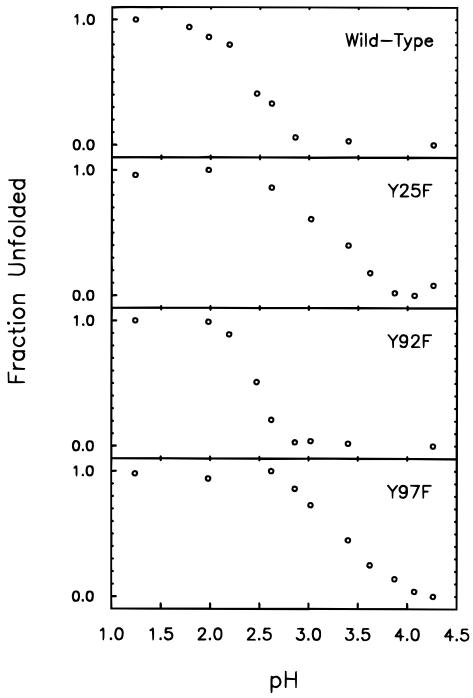

FIGURE 6: pH transition curves of the wild-type protein and the tyrosine-to-phenylalanine mutants of RNase A at 37 °C. For solutions between pH 1.0 and 3.0, the buffer was 0.2 M glycine, and from pH 3.2 to 4.2, the buffer was 0.2 M sodium acetate. The fraction unfolded is calculated from the absorption difference at 287 nm.

indicate that Y25F and Y97F are less stable than the wild-type protein by 1.7 and 2.7 kcal/mol in free energy, respectively, extrapolated to 15 °C and in the absence of denaturant (Table 2). For Y92F, the transition midpoints suggest that the mutant is as stable as the wild-type protein near their folding transitions, although the mutant may be less stable than the wild-type protein at 15 °C and 0 M Gdn·HCl, judging from the decreased transition slopes (ΔH_m and m). However, the kinetic rate constants of Y92F and the wild-type protein are similar, implying that their molecular stabilities are nearly identical (Tables 3−6).

Eberhardt et al. (1996) have measured the thermal transition of Y97F, but under different buffer conditions (0.1 M sodium acetate and 0.1 M sodium chloride at pH 5.0). Their data indicate that Y97F has a transition temperature lower than that of the wild-type protein by approximately 10 °C.

pH transition curves for the unfolding of the wild-type and mutant proteins at 37 °C are shown in Figure 6, and the transition midpoints and differences in proton binding ($\Delta\nu$) are listed in Tables 1 and 2, respectively. At 37 °C and pH 1.2, the unfolding is complete, as was confirmed by raising the temperature to 75 °C. The pH transitions are consistent with the thermal and Gdn·HCl transitions indicating that the Y25F and Y97F mutants are less stable than, while the Y92F mutant is as stable as, the wild-type protein. The value of $\Delta\nu$ for the wild-type protein agrees with the value reported by Yao and Bolen (1995), which is 2.3 H^+ per protein molecule at 25 °C. The values of $\Delta\nu$ suggest that, in both the Y25F and Y97F mutants, an abnormally titrating carboxyl group has become normalized. Interestingly, the Y92F mutation seems to have enhanced the abnormal titration of one or more carboxyl group(s). However, these conclusions must be confirmed by a more careful study of the titrations

Table 3: Parameters Fitting the Single-Jump Unfolding[a] of Wild-Type RNase A and the Tyrosine-to-Phenylalanine Mutants

(A) Time Constants

	fast phase, τ_f (ms)		slow phase, τ_S (s)
	absorption[b]	fluorescence[c]	fluorescence[c]
wild type	41 ± 2	40 ± 1	68 ± 4
Y25F	28 ± 2	29 ± 2	74 ± 3
Y92F	42 ± 3	43 ± 1	42 ± 1
Y97F	16 ± 2	16 ± 2	73 ± 3

(B) Amplitudes

	fast phase, α_f		slow phase, α_S
	absorption[b]	fluorescence[c]	flourescence[c]
wild type	1230 ± 45 (100%)	580 ± 12 (100%)	251 ± 29 (100%)
Y25F	820 ± 45 (67 ± 7%)	464 ± 16 (80 ± 4%)	246 ± 4 (98 ± 12%)
Y92F	1095 ± 45 (89 ± 6%)	476 ± 21 (82 ± 5%)	125 ± 3 (50 ± 12%)
Y97F	685 ± 45 (56 ± 8%)	303 ± 12 (52 ± 4%)	247 ± 11 (98 ± 12%)

[a] The single-jump unfolding was from 1.2 M Gdn·HCl at pH 5.0 to 4.2 M Gdn·HCl at pH 2.0 at 15 °C. The final protein concentration in both the absorption and fluorescence measurements was 0.3 mg/mL. [b] The unfolding was monitored by absorption at 287 nm. The amplitudes are given in arbitrary units. [c] The unfolding was monitored by fluorescence. The excitation wavelength was 268 nm. For emission, a band-pass filter (280−400 nm) was used. The amplitudes (fluorescence increases) are in arbitrary units.

Table 4: Parameters Fitting the Single-Jump Refolding[a] of Wild-Type RNase A and the Tyrosine-to-Phenylalanine Mutants

(A) Time Constants

	τ_f (ms)	τ_m (s)	τ_{SII} (s)	τ_{SI} (s)
wild type	37 ± 2	3.0 ± 0.4	30 ± 1	129 ± 11
Y25F	78 ± 4	3.8 ± 0.2	140 ± 2 s	
Y92F	38 ± 2	2.8 ± 0.4	25 ± 1	156 ± 5
Y97F	2.0 ± 0.3 s		169 ± 3 s	

(B) Amplitudes

	α_f	α_m	α_{SII}	α_{SI}	α_{total}	$\%\alpha_{total}$[b]
wild type	274 ± 21	116 ± 11	737 ± 32	189 ± 21	1316 ± 45	100
Y25F	158 ± 11	74 ± 11	589 ± 11		821 ± 19	62 ± 4
Y92F	200 ± 11	126 ± 11	599 ± 11	273 ± 11	1198 ± 22	91 ± 4
wild type[c]	273 ± 25	149 ± 12	720 ± 25	186 ± 25	1328 ± 45	100
Y97F[c]	186 ± 12		721 ± 12		907 ± 17	68 ± 4

(C) Percentage Amplitudes[d]

	$\%\alpha_f$	$\%\alpha_m$	$\%\alpha_{SII}$	$\%\alpha_{SI}$
wild type	21 ± 1	9 ± 1	56 ± 2	14 ± 1
Y25F	19 ± 1	9 ± 1	72 ± 1	
Y92F	17 ± 1	11 ± 1	50 ± 1	23 ± 1
wild type[c]	21 ± 2	11 ± 1	54 ± 2	14 ± 2
Y97F[c]	21 ± 1		79 ± 1	

[a] The single-jump refolding was from 4.2 M Gdn·HCl at pH 2.0 to 0.6 M Gdn·HCl at pH 5.0 at 15 °C. The refolding was monitored by absorption at 287 nm. The amplitudes are molar absorption increases in arbitrary units. The final protein concentration was 1.3 mg/mL. [b] Value of α_{total} relative to that of the wild type. [c] For the experiments with Y97F, the final protein concentration was 1.1 mg/mL. [d] The percentage amplitudes for each protein were calculated by dividing the fitted amplitude by that protein's α_{total} (part B), multiplied by 100.

of these mutants because of the uncertainties in our determination of $\Delta\nu$.

The pH transition experiment was repeated at 22 °C (data not shown). This indicated that, while the wild-type protein and two of the mutants, Y25F and Y92F, were not completely unfolded at this temperature at pH 1.2, Y97F was completely unfolded. Moreover, the transitions of Y25F and Y92F are not significantly different from that of the wild type, whereas the transition of Y97F was shifted to a higher pH.

Single-Jump Unfolding. The unfolding of the wild-type and mutant proteins consists of two phases, a fast and a slow phase. Their respective time constants and amplitudes are presented in Table 3. It has been shown that the fast phase monitors conformational unfolding (Houry et al., 1994), whereas the slow-phase monitors the cis−trans isomerization of at least one proline (Rehage & Schmid, 1982). The slow phase is detectable only by fluorescence measurements because conformational unfolding has already taken place, exposing the buried tyrosines to solvent; thus, subsequent cis−trans isomerizations affect only the fluorescence, and not absorbance, of nearby tyrosines (Rehage & Schmid, 1982; Schmid et al., 1986; Houry et al., 1994).

For the fast-unfolding phase, the time constants indicate that Y92F unfolds as fast as, while Y25F and Y97F unfold faster than, the wild-type protein (Table 3). This is consistent with the lower stabilities of the latter two determined by the thermal, Gdn·HCl, and pH transitions. The relative absorbance amplitudes of the fast phases of the mutants (Table 3), as compared to those of the wild-type protein, are consistent with $\Delta\epsilon_{287}$ in Table 1. Furthermore, the fluorescence amplitudes indicate that tyrosines 25, 92, and 97

Table 5: Parameters Fitting the Double-Jump Refolding in 0.9 M Gdn·HCl at pH 5.0[a] of Wild-Type RNase A and the Tyrosine-to-Phenylalanine Mutants

(A) Time Constants

	τ_{vf} (ms)	τ_f (ms)	τ_m (s)	τ_{SII} (s)	τ_{SI} (s)
wild type	29 ± 3	61 ± 4	2.4 ± 0.3	43 ± 2	127 ± 18
Y25F	37 ± 3	219 ± 23	2.3 ± 0.4	170 ± 15 s	
Y92F	28 ± 1	64 ± 6	2.2 ± 0.2	38 ± 3	145 ± 22
Y97F	275 ± 12	3.6 ± 0.4 s		206 ± 20 s	

(B) Amplitudes

	α_{vf}	α_f	α_m	α_{SII}	α_{SI}	α_{total}	$\%\alpha_{total}$
wild type	55 ± 96	192 ± 27	96 ± 41	807 ± 27	219 ± 14	1369 ± 112	100
Y25F	41 ± 55	96 ± 14	55 ± 14	642 ± 27		861 ± 76	63 ± 12
Y92F	68 ± 68	123 ± 41	123 ± 41	724 ± 27	191 ± 68	1202 ± 108	88 ± 12
Y97F	14 ± 14	178 ± 14		752 ± 27		944 ± 33	69 ± 9

(C) Percentage Amplitudes[b]

	$\%\alpha_{vf}$	$\%\alpha_f$	$\%\alpha_m$	$\%\alpha_{SII}$	$\%\alpha_{SI}$
wild type	3 ± 3	14 ± 1	7 ± 3	60 ± 3	16 ± 1
Y25F	5 ± 6	12 ± 2	7 ± 2	77 ± 5	
Y92F	7 ± 7	10 ± 3	10 ± 3	59 ± 6	15 ± 5
Y97F	1 ± 1	19 ± 1		80 ± 2	

[a] The refolding step in the double-jump experiments was from 4.2 M Gdn·HCl at pH 2.0 to 0.9 M Gdn·HCl at pH 5.0 at 15 °C. The refolding was monitored by absorption at 287 nm. The final protein concentration was 1.0 mg/mL. The refolding amplitudes (molar absorption increases in arbitrary units) were derived from refolding initiated after the proteins had unfolded for 10 min. [b] The percentage amplitudes for each protein were calculated by dividing the fitted amplitude by that protein's α_{total} (part B), multiplied by 100.

Table 6: Parameters Fitting the Double-Jump Refolding in 1.3 M Gdn·HCl at pH 5.0[a] of Wild-Type RNase A and the Tyrosine-to-Phenylalanine Mutants

(A) Time Constants

	τ_{vf} (ms)	τ_f (ms)	τ_m (s)	τ_S (s)
wild type	80 ± 3	243 ± 18	5.7 ± 0.7	149 ± 3
Y25F	98 ± 7	2.5 ± 0.2 s		273 ± 7
Y92F	75 ± 4	240 ± 15	5.6 ± 0.4	147 ± 2
Y97F	768 ± 15	20 ± 1 s		327 ± 10

(B) Amplitudes

	α_{vf}	α_f	α_m	α_S	α_{total}	$\%\alpha_{total}$
wild type	43 ± 43	260 ± 41	82 ± 14	1081 ± 82	1423 ± 93	100
Y25F	16 ± 57	150 ± 14		670 ± 27	820 ± 30	58 ± 7
Y92F	38 ± 25	191 ± 14	96 ± 27	984 ± 27	1271 ± 41	89 ± 7
Y97F	66 ± 11	164 ± 41		929 ± 68	1093 ± 79	77 ± 10

(C) Percentage Amplitudes[b]

	$\%\alpha_{vf}$	$\%\alpha_f$	$\%\alpha_m$	$\%\alpha_S$
wild type	3 ± 3	18 ± 3	6 ± 1	74 ± 3
Y25F	2 ± 7	18 ± 2		80 ± 6
Y92F	3 ± 2	15 ± 1	7 ± 2	75 ± 2
Y97F	6 ± 1	15 ± 1		80 ± 1

[a] The refolding step in the double-jump experiments was from 4.0 M Gdn·HCl at pH 2.0 to 1.3 M Gdn·HCl at pH 5.0 at 15 °C. The refolding was monitored by absorption at 287 nm. The final protein concentration was 1.0 mg/mL. The refolding amplitudes (molar absorption increases in arbitrary units) were derived from refolding initiated after the proteins had unfolded for 10 min. [b] The percentage amplitudes for each protein were calculated by dividing the fitted amplitude by that protein's α_{total} (part B), multiplied by 100.

contribute to the fluorescence difference between the folded and unfolded protein.

For the slow-unfolding phase, the time constants and amplitudes for Y25F and Y97F are similar to those of the wild-type protein. However, for the Y92F mutant, the time constant is significantly shorter and the amplitude is ~50% lower. This observation for the Y92F mutant has been confirmed by a single-jump unfolding experiment, as well as by manual mixing, with a different starting Gdn·HCl concentration (0.6 M Gdn·HCl at pH 5.0) (data not shown).

The time constants of the slow-unfolding phase of Y92F were measured at various temperatures (Figure 7). The activation energy was determined from an Arrhenius plot to be 22.4 ± 2.8 kcal/mol, which is consistent with proline isomerization (Brandts et al., 1975; Grathwohl & Wüthrich, 1981).

Single-Jump and Double-Jump Refolding. The time constants and absorption amplitudes of the refolding phases were determined for the single-jump refolding experiments (Table 4) and the double-jump experiments (Tables 5 and 6). For the wild-type protein, the data are consistent with those obtained in previous studies (Dodge & Scheraga, 1996; Houry & Scheraga, 1996a). Concerning the mutants, Y92F refolds in a manner similar to that of the wild-type protein,

Table 7: Rate Constants[a] of the New Box Model (Figure 3)

	proline A		proline B		proline C		
	k_1	k_{-1}	k_2	k_{-2}	k_3	k_{-3}	χ^2_{red}
			(A) Unfolding in 4.2 M Gdn·HCl at pH 2.0[b]				
wild type	20.2 ± 1.5	7.7 ± 1.9	12.9 ± 1.0	47.5 ± 4.8	6.7 ± 0.4	2.0 ± 0.3	1.05
	$\tau_1 = 36 \pm 3$		$\tau_2 = 17 \pm 1$		$\tau_3 = 115 \pm 7$		
	$K_1 = 2.6 \pm 0.7$		$K_2^{-1} = 3.7 \pm 0.2$		$K_3 = 3.4 \pm 0.4$		
Y25F	29.0 ± 1.4	14.1 ± 2.4	16.8 ± 2.2	77.4 ± 14.1	7.0 ± 0.3	2.0 ± 0.2	0.96
	$\tau_1 = 23 \pm 2$		$\tau_2 = 11 \pm 2$		$\tau_3 = 111 \pm 5$		
	$K_1 = 2.1 \pm 0.3$		$K_2^{-1} = 4.6 \pm 0.4$		$K_3 = 3.5 \pm 0.3$		
Y92F	24.3 ± 2.2	10.6 ± 3.4	13.3 ± 2.6	52.6 ± 12.0	6.6 ± 0.4	2.0 ± 0.5	0.34
	$\tau_1 = 29 \pm 3$		$\tau_2 = 15 \pm 3$		$\tau_3 = 116 \pm 9$		
	$K_1 = 2.3 \pm 0.6$		$K_2^{-1} = 4.0 \pm 0.2$		$K_3 = 3.3 \pm 0.2$		
Y97F	20.8 ± 1.1	1.4 ± 1.0	369 ± 9020	3057 ± 73000	8.0 ± 0.2	2.0 ± 0.1	0.71
	$\tau_1 = 45 \pm 3$		$\tau_2 = 0.3 \pm 6.4$		$\tau_3 = 99 \pm 3$		
	$K_1 = 14.5 \pm 4.1$		$K_2^{-1} = 8.3 \pm 0.6$		$K_3 = 3.9 \pm 0.2$		
			(B) Unfolding in 4.0 M Gdn·HCl at pH 2.0[c]				
wild type	38.5 ± 2.5	5.5 ± 1.4	14.1 ± 2.6	64.7 ± 14.0	6.5 ± 0.3	2.4 ± 0.3	0.84
	$\tau_1 = 23 \pm 1$		$\tau_2 = 13 \pm 2$		$\tau_3 = 112 \pm 5$		
	$K_1 = 7.0 \pm 2.0$		$K_2^{-1} = 4.6 \pm 0.4$		$K_3 = 2.7 \pm 0.3$		
Y25F	21.5 ± 2.7	2.9 ± 2.2	179 ± 1790	2313 ± 24400	6.7 ± 0.3	1.7 ± 0.2	0.13
	$\tau_1 = 41 \pm 6$		$\tau_2 = 0.4 \pm 204$		$\tau_3 = 119 \pm 6$		
	$K_1 = 7.4 \pm 2.0$		$K_2^{-1} = 12.9 \pm 3.5$		$K_3 = 4.0 \pm 0.4$		
Y92F	32.8 ± 2.6	9.1 ± 1.9	11.3 ± 1.9	47.5 ± 11.0	6.0 ± 0.2	1.7 ± 0.2	0.84
	$\tau_1 = 24 \pm 2$		$\tau_2 = 17 \pm 3$		$\tau_3 = 130 \pm 5$		
	$K_1 = 3.6 \pm 0.6$		$K_2^{-1} = 4.2 \pm 0.4$		$K_3 = 3.5 \pm 0.3$		
Y97F	21.9 ± 1.0	8.1 ± 0.6	3820 ± 4100	50521 ± 54000	9.5 ± 0.1	2.5 ± 0.1	3.48
	$\tau_1 = 33 \pm 2$		$\tau_2 = 0.02 \pm 0.49$		$\tau_3 = 83 \pm 1$		
	$K_1 = 2.7 \pm 0.1$		$K_2^{-1} = 13.2 \pm 0.8$		$K_3 = 3.7 \pm 0.1$		

[a] Rate constants (k's) are in units of 10^{-3} s^{-1} and are defined in Figure 2. τ's and K's are the corresponding time constants (in seconds) and equilibrium constants, respectively. All correspond to a temperature of 15 °C. [b] The refolding conditions for the double-jump experiments are 0.9 M Gdn·HCl at pH 5.0. [c] The refolding conditions for the double-jump experiments are 1.3 M Gdn·HCl at pH 5.0.

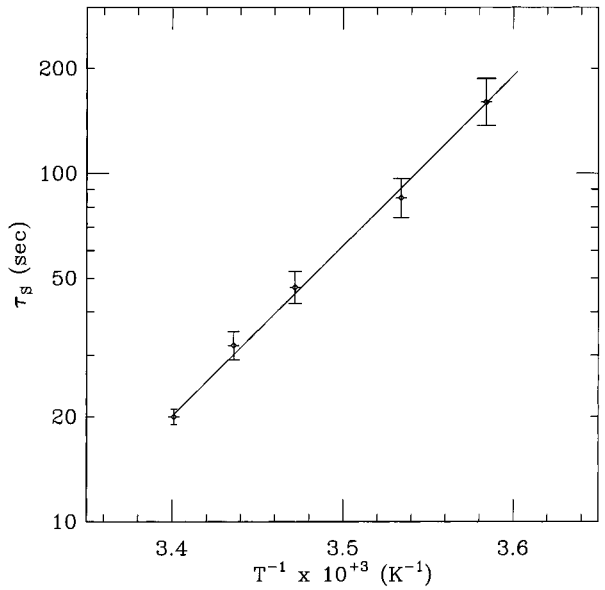

FIGURE 7: Arrhenius plot for the slow fluorescence-monitored unfolding time constant for the Y92F mutant, plotted on a log scale versus inverse temperature. The temperature ranged from 6 to 21 °C. A least-squares fit determined that the activation energy was 22.4 ± 2.8 kcal/mol (95% confidence limit).

while Y25F and Y97F exhibit qualitatively different behavior but resemble each other (Tables 4−6). For the wild-type protein and Y92F in 0.9 M Gdn·HCl at pH 5.0, five refolding phases could be discerned (Table 5). However, in 1.3 M Gdn·HCl at pH 5.0, the two slow phases could not be separated (Table 6) in a statistically meaningful way (Dodge & Scheraga, 1996). These slow phases could also not be separated in the refolding of Y25F and Y97F under all conditions measured. Moreover, in the case of Y97F, the medium phase could not be discerned under all conditions measured. The same was true for Y25F refolding in 1.3 M Gdn·HCl at pH 5.0.

The percentage total amplitudes (%α_{total}) for the refolding of the three mutants (Tables 4B−6B) are consistent with the values of $\Delta\epsilon_{287}$ presented in Table 1. The percentage amplitudes for each refolding phase generally agree with the total amplitude percentages, with some notable exceptions (Tables 4C−6C). For example, the two slow-refolding phases of the wild-type protein seem to combine at high Gdn·HCl concentrations [Table 6 and Dodge and Scheraga (1996)]. For Y97F refolding under all conditions, the medium-refolding phase seems to combine with the slow-refolding phase, judging from the percentage refolding amplitudes. This combination is also observed for Y25F refolding in 1.3 M Gdn·HCl at pH 5.0 (Table 6). For the Y92F mutant refolding in 0.6 M Gdn·HCl at pH 5.0, a small displacement from U_S^{II} to U_S^{I} may have occurred (Table 4). Since these absorption measurements monitor the burial of tyrosines, such combinations probably reflect the disruption of conformational folding (Schmid, 1983).

Box Model of Unfolding. The best-fitting box model for the wild-type, Y25F, and Y92F double-jump data under unfolding conditions is presented in Figure 3. The same best-fit model was arrived at for the six different sets of double-jump data from hundreds of possible models. Its corresponding χ^2 values are much better than those of any competing model, often by a factor of 2 or better (Table 7). By this statistical measure, these fits are preferable to those obtained with a previous box model derived from proline mutant studies [Table 8 and Dodge and Scheraga (1996) and Houry and Scheraga (1996a)]. Moreover, the equilibrium constants K and time constants τ are consistent with cis−

Table 8: Rate Constants[a] Fitted to the Previous Box Model (Houry et al., 1994; Dodge & Scheraga, 1996; Houry & Scheraga, 1996a)

	k_1	k_{-1}	k_2	k_{-2}	k_3	k_{-3}	χ^2_{red}
			(A) Unfolding in 4.2 M Gdn·HCl at pH 2.0[b]				
wild type	20.2 ± 1.2	1.9 ± 0.4	2.6 ± 0.8	8.9 ± 3.1	11.0 ± 0.5	2.7 ± 0.3	2.41
	$\tau_1 = 45 \pm 3$		$\tau_2 = 87 \pm 24$		$\tau_3 = 73 \pm 3$		
	$K_1 = 10.6 \pm 2.5$		$K_2^{-1} = 3.4 \pm 0.3$		$K_3 = 4.1 \pm 0.3$		
Y92F	21.7 ± 1.2	1.3 ± 0.6	3.2 ± 1.1	12.1 ± 5.4	9.3 ± 0.6	2.2 ± 0.5	1.34
	$\tau_1 = 43 \pm 3$		$\tau_2 = 65 \pm 24$		$\tau_3 = 87 \pm 6$		
	$K_1 = 16.7 \pm 1.9$		$K_2^{-1} = 3.8 \pm 0.6$		$K_3 = 4.2 \pm 0.9$		
			(B) Unfolding in 4.0 M Gdn·HCl at pH 2.0[c]				
wild type	32.1 ± 3.5	2.5 ± 0.6	130.8 ± 1775	1219 ± 18874	8.5 ± 0.5	2.6 ± 0.4	1.47
	$\tau_1 = 29 \pm 3$		$\tau_2 = 1 \pm 10$		$\tau_3 = 90 \pm 5$		
	$K_1 = 12.8 \pm 2.8$		$K_2^{-1} = 9.3 \pm 2.5$		$K_3 = 3.3 \pm 0.3$		
Y92F	23.8 ± 5.2	2.4 ± 0.8	95.6 ± 343	934 ± 3556	8.5 ± 0.5	1.9 ± 0.2	1.03
	$\tau_1 = 38 \pm 8$		$\tau_2 = 1 \pm 3$		$\tau_3 = 96 \pm 5$		
	$K_1 = 9.9 \pm 1.9$		$K_2^{-1} = 9.8 \pm 3.4$		$K_3 = 4.5 \pm 0.4$		

[a] See the explanations in Table 7. [b] See the explanations in Table 7. [c] See the explanations in Table 7.

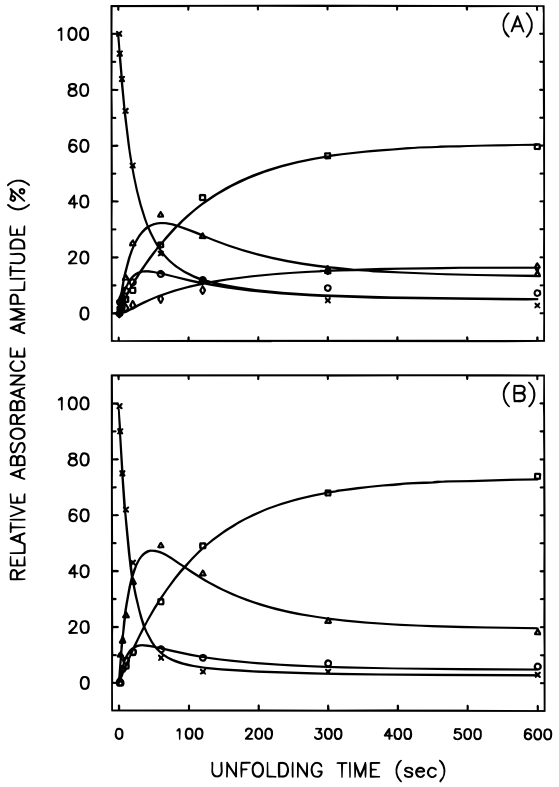

FIGURE 8: Relative amplitudes of the different refolding phases of the wild-type protein at different unfolding times in the double-jump experiments. (A) Unfolding was carried out in 4.2 M Gdn·HCl at pH 2.0, and refolding was in 0.9 M Gdn·HCl at pH 5.0 and 15 °C (Table 5). (B) Unfolding and refolding were carried out in 4.0 M Gdn·HCl at pH 2.0 and 1.3 M Gdn·HCl at pH 5.0, respectively, at 15 °C (Table 6). The symbols ×, △, ○, □, and ◇ represent the experimental points corresponding to the very fast-, fast-, medium-, minor slow-, and major slow-(or slow-) refolding phases, respectively; the solid lines are the theoretical curves determined by the improved box model (Figure 3 and Table 7).

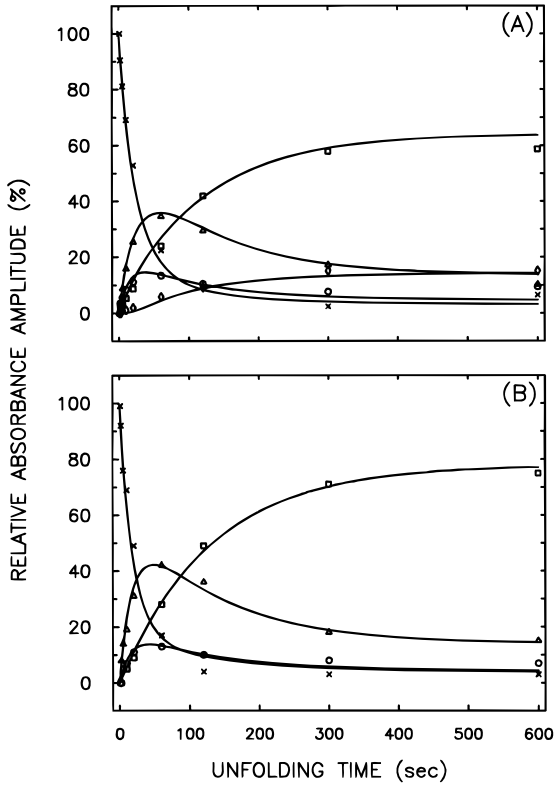

FIGURE 9: Relative amplitudes of the different refolding phases of Y92F at different unfolding times in the double-jump experiments. See Figure 8 for explanations.

trans isomerization of X−Pro peptide bonds [Table 7 and Brandts et al. (1975) and Grathwohl and Wüthrich (1981)]. The rate curves for the wild-type protein and the Y92F mutant are presented in Figures 8 and 9, respectively. For the Y97F mutant under unfolding conditions, a similar box model is slightly superior to the box model of Figure 3; the only difference is that the species U_4 was associated with U_S instead of U_m, as in the wild-type box model. The χ^2 values of these two box models are very close but almost 4-fold better than that of the nearest competing box model.

For this study, we make the working assumption that the model of Figure 3 faithfully represents the proline isomerization kinetics of wild-type RNase A under unfolding conditions.

The rate, time, and equilibrium constants for all eight sets of double-jump data are presented in Table 7. Although the rate constants in parts A and B of Table 7 generally agree, there are some discrepancies. The rate constants in Table 7A are considered more reliable because more refolding phases could be discerned than for the fits in Table 7B. Some rate constants of the box model for the Y25F and Y97F mutants have large statistical errors, because only three refolding phases were discerned; their formal best-fit values (in the physically implausible millisecond range) are presented merely for completeness.

For the wild-type protein, the best-fitting box model shows the following features (Figure 3). The proline isomerization

corresponding to k_1 and k_{-1} is reasonably rapid, corresponding to a time constant of 36 s (Table 7A). This proline (denoted A) is cis in its native state, since its equilibrium constant K_1 equals 2.6 (Table 7A), consistent with a cis−trans equilibrium (Grathwohl & Wüthrich, 1981). The isomerization of proline A distinguishes the species U_1 and U_2 (Figure 2) and thus the U_{vf} and U_f refolding phases (Figure 3). The proline isomerization corresponding to k_2 and k_{-2} is very rapid, corresponding to a time constant of 17 s (Table 7A). This proline (denoted B) is trans in its native state, since its equilibrium constant equals 1/3.7 (Table 7A), consistent with a trans−cis equilibrium (Grathwohl & Wüthrich, 1981). This isomerization distinguishes the species U_1 and U_2 from U_3 and U_4 (Figure 2) and thus the fast-refolding phases U_{vf} and U_f from the medium-refolding phase U_m (Figure 3). The isomerization of proline B also distinguishes the species U_5 and U_6 from U_7 and U_8 (Figure 2) and thus the major slow-refolding species U_S^{II} from the minor slow-refolding species U_S^{I} (Figure 3). The proline isomerization corresponding to k_3 and k_{-3} is slow, corresponding to a time constant of 115 s (Table 7A). This proline (denoted C) is cis in its native state, judging from its equilibrium constant of 3.4 (Table 7A), by analogy with proline A (Grathwohl & Wüthrich, 1981). This isomerization distinguishes the species U_1-U_4 from U_5-U_8 (Figure 2) and hence the slow-refolding species U_S^{II} and U_S^{I} from the fast- and medium-refolding phases (Figure 3). These properties are also observed in the box model fits of double-jump data taken under different unfolding and refolding conditions for the wild-type protein (compare parts A and B of Table 7).

For the Y92F mutant, the rate constants of the best-fitting box model are generally similar to those of the wild-type protein (Table 7A). However, under the unfolding conditions of 4.0 M Gdn·HCl at pH 2.0, some differences can be noted (Table 7B). For the isomerization of proline A, the equilibrium constants are significantly different. The wild-type protein shows a surprisingly large equilibrium constant of 7.0, whereas the Y92F mutant has an equilibrium constant of 3.6, which is more consistent with proline isomerization [Table 7B and Grathwohl and Wüthrich (1981)]. This discrepancy corresponds to a *z*-score of 1.6, corresponding to an 11% probability of such a large discrepancy arising by chance. Second, the time constant of proline C is significantly longer in the Y92F mutant (130 s) than in the wild-type protein (112 s) (Table 7B). This discrepancy appears to be more significant, corresponding to a *z*-score of 2.5 and thus a 1% chance probability. A similar acceleration has been observed in model peptide studies where the equilibrium constant for the cis−trans isomerization of the Tyr−Pro peptide bond is nearly identical to that of the Phe−Pro peptide bond but the rate constants are roughly 2-fold faster (Grathwohl & Wüthrich, 1981).

It should be noted that all such box models may neglect some essential folding processes, e.g. cooperativity between the X−Pro peptide bonds and isomerization about disulfide bonds (Mui et al., 1985) and about other X−Y peptide bonds for which Y is not a proline residue (Dodge & Scheraga, 1996; Houry & Scheraga, 1996a). This neglect may lead to poor fits and spurious rate constants.

DISCUSSION

Tyrosine Contributions to Absorption Amplitudes. The values of $\Delta\epsilon_{287}$ for the mutants Y25F and Y97F are consistent with previous studies (Bigelow, 1961; Woody et al., 1966) and indicate that tyrosines 25 and 97 each contribute roughly 1000 M^{-1} cm^{-1} to the absorption difference at 287 nm, consistent with the conclusion that these tyrosines are completely buried in the native state. This conclusion is supported by structural data determined by X-ray crystallography, NMR spectroscopy, and other physical and biochemical studies (Woody et al., 1966; Wlodawer et al., 1988; Santoro et al., 1993). In contrast, tyrosine 92 seems to be only partially buried, contributing roughly 367 ± 166 M^{-1} cm^{-1}. It should be noted that this value is significantly smaller than the previously reported value of 700 M^{-1} cm^{-1} (Bigelow, 1961). This discrepancy may indicate the presence of at least one other partially buried tyrosine residue. However, the sum of the three contributions is 2478 ± 272 M^{-1} cm^{-1}, which agrees, within experimental error, with the total absorption difference of wild-type RNase A (2749 ± 127 M^{-1} cm^{-1}). The *z*-score is 1.8, corresponding to a 9% probability of such a large discrepancy arising by chance. Thus, the conclusion that a fourth tyrosine is responsible for the discrepancy in the difference spectrum is supported only by weak statistical evidence.

Effects of the Mutations on the Molecular Stability and Enzymatic Activity. The two mutations, in Y25F and Y97F, significantly affect the enzymatic activity and molecular stability of ribonuclease A, consistent with the burial of tyrosines 25 and 97. These tyrosines probably influence the enzymatic activity and molecular stability through the interactions of their hydroxyl groups with neighboring residues, including aspartates 14 and 83 and lysine 41 (Li et al., 1966; Scheraga, 1967; Eberhardt et al., 1996). In particular, the interactions with tyrosine 97 are known to be strong, even surviving thermal denaturation at neutral pH (Bigelow, 1961), possibly because of their burial in a low-dielectric hydrophobic environment; X-ray and NMR data indicate that the second helix of RNase A packs against the β-sheet region containing Tyr97 (Wlodawer et al., 1988; Santoro et al., 1993). Similarly, tyrosine 25 may influence the formation of the first helix through its interaction with aspartate 14, as well as active site residue His12 (Wlodawer et al., 1983).

In contrast, tyrosine 92 does not seem to stabilize the protein significantly, in agreement with other data from this laboratory (Burgess & Scheraga, 1975; Sendak et al., 1996). A study of the tyrosine-to-tryptophan mutant Y92W indicates that this mutation does not result in a significant loss of enzymatic activity or molecular stability as determined by thermal and Gdn·HCl transitions (Sendak et al., 1996). In addition, denaturation kinetic measurements indicate that normalization of the pK_a of the hydroxyl group of tyrosine 92 by lowering the pH alters the UV difference spectrum at 287 nm but not at 235 nm, suggesting that the normalization does not alter the backbone conformation in the region around tyrosine 92 (Scott & Scheraga, 1963; Burgess & Scheraga, 1975). Therefore, the hydroxyl group of tyrosine 92 is not essential for the enzymatic activity and structural stability of ribonuclease A.

These observations are consistent with the effects of these mutations on the fast unfolding of RNase A. Replacing tyrosine 25, and especially tyrosine 97, with phenylalanine strongly accelerates the conformational unfolding (Table 3). In contrast, the Y92F mutation does not affect the fast unfolding (Table 3). It is worth noting that the converse is

also observed for conformational refolding; e.g. the Y97F mutation strongly decelerates conformational refolding (see below).

The fluorescence amplitude of the slow-unfolding phase corresponds to the *local* fluorescence change of the tyrosine residues, which may arise from the cis−trans isomerization of nearby X−Pro peptide bonds (Rehage & Schmid, 1982; Sendak et al., 1996). The dramatic drop in the fluorescence amplitude for the slow-unfolding phase of Y92F (Table 3) indicates that tyrosine 92 contributes half of the fluorescence amplitude of the slow unfolding phase of wild-type RNase A, which is presumably due to the cis−trans isomerization of the X−Pro93 peptide bond (Sendak et al., 1996). However, the fluorescence amplitude of the slow-unfolding phase of Y92F is still ∼50% of the wild-type amplitude, suggesting that at least one other tyrosine residue is involved (Table 3). This other tyrosine also monitors a proline isomerization, judging from its activation energy of 22.4 ± 2.8 kcal/mol. Since the protein is already conformationally unfolded (Houry et al., 1994), and only tyrosines 92 and 115 are adjacent to prolines, the most likely candidate is tyrosine 115, whose fluorescence properties may monitor the cis−trans isomerization of the X−Pro114 peptide bond. This hypothesis is supported by the observation that the slow unfolding time constant of Y92F ($\tau_S = 42 \pm 1$ s in Table 3) agrees with the isomerization time constant ($\tau_1 = 36 \pm 3$ s in Table 7A) of an essential proline (tentatively identified below as Pro114) of wild-type RNase A.

These observations contradict the conclusions of Schmid et al. (1986), who proposed that tyrosine 92 is solely responsible for the slow fluorescence-unfolding phase. In particular, they observed that the slow fluorescence-unfolding phase is absent in guinea pig pancreatic ribonuclease A, in which a phenylalanine is also substituted for tyrosine 92 but Pro114 and Tyr115 are unchanged (Blackburn & Moore, 1982). This discrepancy may result from differences in experimental conditions and the amino acid sequence. Under the conditions of Schmid et al. (1986), the protein concentration ranged from 3 to 5 μM, while in this study, the concentration of Y92F used was 20 μM; therefore, a stronger fluorescence signal was obtained. It should also be noted that guinea pig RNase A has 33 amino acid substitutions compared to bovine RNase A (Blackburn & Moore, 1982). In particular, the X residue of X−Pro114 in bovine pancreatic RNase A is Asn113 while that in guinea pig pancreatic RNase A is Lys113 (Blackburn & Moore, 1982). This sequence difference may possibly explain the absence of a slow-unfolding phase in guinea pig RNase A.

The slow-unfolding phases of the Y25F and Y97F mutants are similar to that of wild-type RNase A in terms of the fluorescence amplitude and time constant. This indicates that tyrosines 25 and 97 do not contribute to the fluorescence change observed in the slow-unfolding phase, as suggested previously (Schmid et al., 1986).

Roles of Tyrosines 25 and 97 in Conformational Refolding. The stopped-flow single-jump refolding absorbance measurements indicate that tyrosines 25 and 97 are involved in interactions that accelerate the conformational folding in the wild-type protein. When these tyrosines are removed in the mutants Y25F and Y97F, the refolding time constants become significantly larger under various solution conditions (Tables 4A−6A). It has been established that the refolding of U_{vf}, U_f, U_m, and U_S^{II} (as detected by absorption) is not rate-limited by proline isomerization, but by conformational folding (Houry & Scheraga, 1996a). Therefore, the deceleration of these refolding phases, relative to the wild type, in tyrosine-to-phenylalanine mutants suggests that the corresponding tyrosines are involved in interactions crucial to conformational folding. Judging from these decelerations, tyrosine 97 strongly influences the refolding of U_{vf} and U_f; this is also true to a lesser extent for tyrosine 25 (Tables 4A−6A). Moreover, the major slow-refolding phase U_S^{II} combines with the minor slow-refolding phase U_S^{I} for both mutants; since U_S^{II} is distinguished from U_S^{I} by the folding step $U_S^{II} \rightarrow I_N$, tyrosines 25 and 97 seem to be essential to this conformational folding reaction (Schmid, 1983). The effects of these mutations on the medium-refolding phase U_m are more uncertain but generally indicate that these mutations also decelerate this refolding phase (Tables 4A−6A). Therefore, tyrosine 25, and especially tyrosine 97, seem to be crucial in the conformational refolding of RNase A.

The roles of tyrosines 25 and 97 in the conformational refolding can be explained, at least partly, in terms of their stabilizing interactions in the intermediates on the refolding pathway. In particular, the refolding of U_{vf} has been studied by H−D exchange and the structure of the intermediate I_Φ elucidated (Houry & Scheraga, 1996b). In this intermediate, the major β-hairpin (residues 83−100) seems to be formed already, and Tyr97 seems to be buried by the second helix (Houry & Scheraga, 1996b). Tyrosine 25 also appears to be buried, but not aspartate 14 (Houry & Scheraga, 1996b). The carboxy-terminal region (residues 47−82 and 106−124) seems to be largely disordered (Houry & Scheraga, 1996b). Hence, the hydroxyl groups of tyrosines 25 and 97 seem to stabilize the ordered structure in the I_Φ intermediate, i.e. the major β-hairpin and the second helix. Similarly, the absence of a U_S^{II} refolding phase in the Y25F and Y97F mutants can be explained by the destabilization of the I_N intermediate (Schmid, 1983). Since it is known that I_N is structurally similar to the native species (Udgaonkar & Baldwin, 1988, 1990, 1995), presumably, the native interactions of tyrosines 25 and 97 are also present in this intermediate, which may explain the destabilization of both I_N and N by these tyrosine-to-phenylalanine mutations.

Tyrosines 25 and 97 seem to play a particularly important role in the fast-refolding phase U_f, judging by the rate constants of the Y25F and Y97F mutants compared to those of the wild-type protein. This is especially true for tyrosine 97, which seems to be responsible for a roughly 50−80-fold acceleration of the fast-refolding phase (Tables 4−6). This correlates well with studies indicating that the conformational unfolding and refolding of U_f are extremely pH-dependent; the refolding rate increases, and the unfolding rate decreases, by a factor of 200 as the pH is increased from 2.0 to 5.0 and corresponds to the titration of a carboxyl group (Dodge & Scheraga, 1996; Sendak et al., 1996; Houry & Scheraga, 1996a). Similarly, the thermal transition temperature of RNase A is strongly pH-dependent, following the titration of a carboxyl group (Hermans & Scheraga, 1961a). Thus, the deceleration of the fast-refolding phase and our pH transition studies suggest that the influence of tyrosines 25 and 97 on the conformational folding and molecular stability may be mediated by interactions with carboxylate groups (Scheraga, 1957, 1967, 1984).

Interestingly, the relative influence of these tyrosyl interactions on the refolding of U_f seems to increase with increasing

Gdn·HCl concentrations. The time constant τ_f for Y25F, relative to the wild-type protein, increases from roughly 2- to 10-fold, as the refolding Gdn·HCl concentration increases from 0.6 to 1.3 M (Tables 4A−6A). Similarly, the time constant for Y97F increases from 50- to 80-fold under the same conditions (Tables 4A−6A). This deceleration may reflect the relative importance of the tyrosyl interactions, although a more thorough investigation of the U_f refolding pathway is required to interpret this Gdn·HCl dependence.

Roles of Tyrosines 25 and 97 in Proline Isomerization. Tyrosines 25 and 97 also influence the isomerization of the X−Pro peptide bond(s) which is rate-limiting for the slow-refolding phases (Tables 4A−6A; Schmid, 1983; Schmid et al., 1986). For example, in 1.3 M Gdn·HCl, the time constant for the U_S^I refolding phase of Y97F is over twice as large as that of the wild-type protein. It is argued below that the isomerization of Pro93 is rate-limiting for the slow-refolding phases. As in conformational folding, tyrosines 25 and 97 may accelerate the isomerization of the X−Pro93 peptide bond by stabilizing the β-hairpin in which Pro93 lies.

The relative importance of these tyrosyl interactions for this isomerization also increases with increasing Gdn·HCl concentrations. These acceleration factors are relatively small, ranging from 1.3 to 2.2-fold increases; nonetheless, they are statistically significant.

Box Model for Unfolding Isomerizations. The arrangement of the refolding phases in the best-fitting box model (Figure 3) differs in three respects from that of a previous box model (Dodge & Scheraga, 1996; Houry & Scheraga, 1996a). First, in the new model, the fast phase U_f is associated with only one species, whereas in the previous model, U_f was associated with two species, differing in two proline isomerizations (Figure 3). Second, the medium-refolding phase U_m in the new model is associated with two adjacent species, whereas in the previous model, the medium phase was associated with two species on opposite corners of the box, differing from each other in three proline isomerizations (Figure 3). Finally, the slow-refolding phases U_S^{II} and U_S^I are each associated with two adjacent species in the new model, with U_S^{II} parallel to the fast- and very fast-refolding phases and U_S^I parallel to the medium-refolding phases. In the previous model, U_S^{II} was associated with two species separated by two proline isomerizations; U_S^I was associated with a *single* species on the corner most distant from U_{vf} (Figure 3).

The new box model yields a much better χ^2 than the previous model. As an example, for the wild-type double-jump refolding data in 0.9 M Gdn·HCl at pH 5.0, the previous box model ranked 35th of the models tested, with a χ^2 well over twice that of the new box model. Moreover, the fitted equilibrium and time constants of the new model are physically plausible and consistent with the hypothesis of proline isomerization [Table 7 and Brandts et al. (1975) and Grathwohl & Wüthrich (1981)], which is not true in the previous box model [Table 8 and Dodge and Scheraga (1996) and Houry and Scheraga (1996)]. Lastly, similar refolding phases are associated with adjacent species in the new box model which is not true of the previous box model; for example, U_m was associated with two species separated by three proline isomerizations (Dodge & Scheraga, 1996).

The following elucidates some reasons for the improved χ^2 value. The new assignment of U_f correlates better with the experimentally observed 25:75 ratio in the U_{vf}:U_f refolding amplitudes (Houry et al., 1994) and, thus, with the hypothesis of proline isomerization (Brandts et al., 1975; Grathwohl & Wüthrich, 1981). The previous assignment of refolding phases required a physically implausible equilibrium constant of roughly 10 along one direction of the box [Table 8 and Dodge and Scheraga (1996) and Houry and Scheraga (1996a)]. Second, the previous model had no direct unfolding reaction from U_{vf} to any of the slow phases; therefore, the slow phases should exhibit a lag under unfolding conditions. Such a lag is not observed; the buildup of the slow-refolding phases seems to follow a simple exponential.

Assignment of Prolines to the Box Model. The crucial remaining task is assignment of the three essential prolines of RNase A (Pro93, Pro114, and Pro117) to the three prolines of the box model (prolines A, B, and C). In this paper, we propose that proline A corresponds to Pro114, that proline B corresponds to Pro117, and that proline C corresponds to Pro93, for the following reasons.

The assignment of proline B to Pro117 is relatively straightforward, since its fitted equilibrium constant K_2 indicates that it is trans in the native state and Pro117 is the only essential trans proline in RNase A (Dodge et al., 1994; Dodge & Scheraga, 1996). Moreover, Pro117 occurs near the carboxy terminus of the protein, which is known to be very mobile. This is consistent with the observation that the fitted rate constants k_2 and k_{-2} are significantly higher than the other isomerization rate constants for the wild-type and mutant proteins. However, the assignments of prolines A and C are not so simple, since their fitted equilibrium constants indicate that they are both cis in the native state.

Several arguments support the assignments of Pro114 to proline A and Pro93 to proline C. First, the slow fluorescence-unfolding phase of the Y92F mutant has a time constant of 42 ± 1 s (Table 3), which agrees reasonably with the fitted time constant τ_1 of proline A (36 ± 3 s) and poorly with the fitted time constant τ_3 of proline C (115 ± 7 s) of the wild-type protein (Table 7A). If indeed the slow fluorescence-unfolding phase of the Y92F mutant reflects the fluorescence change of tyrosine 115 as proline 114 undergoes cis−trans proline isomerization, then proline A corresponds to proline 114. As a further check, the slow-unfolding fluorescence signal of Y92F was subtracted from that of the wild-type to estimate the slow-unfolding fluorescence signal contributed by tyrosine 92. Fitting this estimated fluorescence signal yielded a single decaying exponential with a time constant of 92 s, which agrees well with the fitted time constant of proline C (115 ± 7 s) and poorly with that of proline A (36 ± 3 s). This supports the identification of proline C as proline 93. Third, tyrosines 25 and 97 were shown above to accelerate the isomerization of the slow-refolding phases, which correspond to the isomerization of proline C in the improved box model (Tables 4A−6A). Since these tyrosines were shown above to stabilize the ordered structure near the β-hairpin involved in conformational folding, this acceleration supports the assignment of proline C to Pro93 which is located in this hairpin. This correlation is supported by the recent suggestion that the X−Ala93 peptide bond of the P93A mutant is stabilized by conformational forces and remains cis in the folded structure (Dodge & Scheraga, 1996). Lastly, this assignment of prolines agrees with the double-jump data taken on proline mutants of RNase A (Dodge & Scheraga, 1996).

The previous box model was proposed to fit the double-jump data of several proline-to-alanine mutants, notably P93A, P114A, and P117A (Dodge & Scheraga, 1996). However, the previous model did not result from exhaustive statistical modeling, i.e. choosing the best-fitting model from among all possible assignments of refolding phases to the different isomerization species, as carried out in this study. We re-examined the previous data for each proline-to-alanine mutant using the technique of exhaustive fitting to all possible two-proline models. For such mutants, only two prolines should be essential for two reasons. First, Pro42 was shown to be nonessential in the wild-type protein (Dodge et al., 1994; Dodge & Scheraga, 1996), and we assume that Pro42 remains nonessential in these mutants. Second, the X−Ala peptide bond associated with the substituted alanine does not isomerize in the range of unfolding times in our double-jump experiments. On the one hand, Ala114 and Ala117 do not seem to isomerize under unfolding conditions, remaining trans, and on the other, the isomerization of Ala93 [suggested to be cis in the folded state (Dodge & Scheraga, 1996)] to trans seems to be complete before our double-jump experiments initiate refolding.

The best-fit two-proline models support the new box model proposed here both in the assignment of refolding phases and in their equilibrium and time constants. In particular, the P117A mutant was well fit by the new box model, which was not true for the previous box model (Dodge & Scheraga, 1996; Houry & Scheraga, 1996a). The new fitted isomerization time constants are 28 ± 2 and 84 ± 3 s, which agree reasonably well with the respective values for prolines A and C in this study (Table 7A). This supports our identification of proline B as Pro117. For the P114A mutant, the slower isomerization time constant is 93 ± 4 s, which agrees with the present value for proline C (Table 7A); this supports the identification of Pro114 as proline A. For the P93A mutant, the slower isomerization time constant was 45 ± 2 s, which agrees with the present value for proline A (Table 7A), supporting the identification of Pro93 as proline C. Further details of these exhaustive fittings and the assignment of prolines to the box model will be discussed in a forthcoming paper.

Interpretation of the New Box Model. Since our kinetic data implicate Pro93 as being responsible for the slow *unfolding* of RNase A, Pro93 is presumably also responsible for the slow *refolding* reactions $U_S^I \rightarrow N$ and $I_N \rightarrow N$, which have been shown to be rate-limited by the cis−trans isomerization of a proline (Schmid, 1983; Schmid et al., 1986). In particular, the species U_5 of the box model (Figure 2) refolds as U_S^{II} whose refolding involves the $I_N \rightarrow N$ reaction (Schmid, 1983; Schmid et al., 1986). However, this species has only proline C, assigned here as Pro93, in a non-native isomer. The conclusion that Pro93 is responsible for the slow-refolding reactions is also supported by single-jump refolding experiments on the Y92W mutant (Sendak et al., 1996).

The parallel assignment of the refolding phases in the new model is striking. For example, the folding phases are identical along the proline A direction of the box, with the exception of U_{vf} and U_f. Hence, the isomeric state of proline A (assigned here as Pro114) does not affect the refolding transition state(s) of these phases significantly. This correlates well with several theoretical and experimental studies showing that a non-native Pro114 does not perturb the native conformation or interfere with the refolding of RNase A significantly (Stimson et al., 1982; Pincus et al., 1983; Oka et al., 1984; Montelione et al., 1984; Ihara & Ooi, 1985; Schultz et al., 1992; Dodge & Scheraga, 1996). It should also be noted that the U_{vf} refolding phase is absent in the P114A mutant (Dodge & Scheraga, 1996), consistent with the new box model (Figure 3).

From measurements of activation energies, it has been shown that the refolding phases, U_{vf}, U_f, and U_m, as well as the reaction $U_S^{II} \rightarrow I_N$, are rate-limited by conformational folding (Houry & Scheraga, 1996a), whereas the refoldings of I_N and U_S^I are rate-limited by proline isomerization (Schmid, 1983; Schmid et al., 1986; Houry & Scheraga, 1996a). According to the best-fit box model, proline A (Pro114) distinguishes the fast- and very fast-refolding phases, proline B (Pro117) distinguishes the medium- from the fast- and very fast-refolding phases, and proline C (Pro93) distinguishes the slow-refolding phases from the fast-, very fast- and medium-refolding phases. Thus, since the conformational refolding rates of U_f, U_m, and U_S^{II} are progressively slower, the best-fit box model indicates that non-native isomeric states of prolines 114, 117, and 93 cause increasing disruption of conformational folding. In particular, conformational folding in advance of proline isomerization is impossible for any species with both prolines 117 and 93 in non-native isomeric states (i.e. U_S^I). These tendencies are consistent with the known structures of the conformational refolding intermediates (Udgaonkar & Baldwin, 1988, 1990, 1995; Houry & Scheraga, 1996b).

CONCLUSIONS

This study confirms that tyrosines 25, 92, and 97 contribute most of the absorption and fluorescence differences between the folded and unfolded protein, although a fourth tyrosine cannot be ruled out. The absorption differences at 287 nm indicate that tyrosines 25 and 97 are completely buried in the native protein, whereas tyrosine 92 is only partially buried.

Tyrosines 25 and 97 seem to be involved in interactions that accelerate conformational folding as well as the isomerization of proline 93. These interactions seem to stabilize the major β-hairpin structure of the native state and several folding intermediates. Moreover, the interactions of tyrosines 25 and 97 with nearby carboxylate groups may contribute to the strong pH-dependence of the folding/unfolding kinetics, especially of U_f, and of the thermal transition temperature (Hermans & Scheraga, 1961a).

The Y92F mutation does not result in a significant loss of molecular stability or enzymatic activity, suggesting that the interaction of the hydroxyl group of tyrosine 92 and the carboxylate group of aspartate 38 is weak, supporting previous studies (Burgess & Scheraga, 1975; Sendak et al., 1996).

Our study suggests that tyrosines 92 and 115 both contribute to the slow fluorescence-unfolding phase, contradicting the conclusion from previous studies (Schmid et al., 1986). Activation energy measurements and the fitted isomerization time constant of Pro114 indicate that the fluorescence properties of tyrosine 115 may monitor the cis−trans isomerization of the X−Pro114 peptide bond.

Exhaustive fitting of the double-jump data to all possible box models yielded an improved model for RNase A.

Comparison of the box models generally indicates that tyrosine 92 does not significantly influence the rates of the cis−trans isomerizations of Pro93, Pro114, and Pro117 under *unfolding* conditions. The kinetic data support the identification of Pro93 as the proline whose isomerization distinguishes the slow-*refolding* species (U_S^{II} and U_S^{I}) from the other faster-refolding species (U_{vf}, U_f, and U_m), implicating Pro93 in the slow refolding reactions $U_S^{I} \rightarrow N$ and $I_N \rightarrow N$. Similarly, Pro114 seems to distinguish the very fast-refolding species U_{vf} and the fast-refolding species U_f. Lastly, Pro117 seems to distinguish the major slow-refolding species U_S^{II} from the minor slow-refolding species U_S^{I} and the medium-refolding species U_m from the fast- and very fast-refolding species.

ACKNOWLEDGMENT

We thank R. W. Dodge, W. A. Houry, N. L. Kelleher, and D. M. Rothwarf for suggestions and assistance throughout this study and the Cornell Theory Center for computer resources. The Cornell Theory Center is funded in part by the National Science Foundation, the State of New York, the IBM Corp., and members of the Corporate Research Institute, as well as by special support for the Parallel Processing Resource for Biomedical Scientists from the National Center for Research Resources of the National Institutes of Health.

REFERENCES

Adler, M., & Scheraga, H. A. (1990) *Biochemistry 29*, 8211−8216.
Baker, W. R., & Kintanar, A. (1996) *Arch. Biochem. Biophys. 327*, 189−199.
Bigelow, C. C. (1961) *J. Biol. Chem. 236*, 1706−1710.
Blackburn, P., & Moore, S. (1982) *Enzymes 15*, 317−433.
Brandts, J. F., Halvorson, H. R., & Brennan, M. (1975) *Biochemistry 14*, 4953−4963.
Burgess, A. W., & Scheraga, H. A. (1975) *J. Theor. Biol. 53*, 403−420.
Cook, K. H., Schmid, F. X., & Baldwin, R. L. (1979) *Proc. Natl. Acad. Sci. U.S.A. 76*, 6157−6161.
Crook, E. M., Mathias, A. P., & Rabin, B. R. (1960) *Biochem. J. 74*, 234−238.
delCardayré, S. B., Ribó, M., Yokel, E. M., Quirk, D. J., Rutter, W. J., & Raines, R. T. (1995) *Protein Eng. 8*, 261−273.
Denton, J. B., Konishi, Y., & Scheraga, H. A. (1982) *Biochemistry 21*, 5155−5163.
Dodge, R. W., & Scheraga, H. A. (1996) *Biochemistry 35*, 1548−1559.
Dodge, R. W., Laity, J. H., Rothwarf, D. M., Shimotakahara, S., & Scheraga, H. A. (1994) *J. Protein Chem. 13*, 409−421.
Eberhardt, E. S., Wittmayer, P. K., Templer, B. M., & Raines, R. T. (1996) *Protein Sci. 5*, 1697−1703.
Garel, J.-R., & Baldwin, R. L. (1973) *Proc. Natl. Acad. Sci. U.S.A. 70*, 3347−3351.
Garel, J.-R., & Baldwin, R. L. (1975) *J. Mol. Biol. 94*, 611−620.
Garel, J.-R., Nall, B. T., & Baldwin, R. L. (1976) *Proc. Natl. Acad. Sci. U.S.A. 73*, 1853−1857.
Grathwohl, C., & Wüthrich, K. (1981) *Biopolymers 20*, 2623−2633.
Hermans, J., Jr., & Scheraga, H. A. (1961a) *J. Am. Chem. Soc. 83*, 3283−3292.
Hermans, J., Jr., & Scheraga, H. A. (1961b) *J. Am. Chem. Soc. 83*, 3293−3300.
Houry, W. A., & Scheraga, H. A. (1996a) *Biochemistry 35*, 11719−11733.
Houry, W. A., & Scheraga, H. A. (1996b) *Biochemistry 35*, 11734−11746.
Houry, W. A., Rothwarf, D. M., & Scheraga, H. A. (1994) *Biochemistry 33*, 2516−2530.
Houry, W. A., Rothwarf, D. M., & Scheraga, H. A. (1995) *Nat. Struct. Biol. 2*, 495−503.
Ihara, S., & Ooi, T. (1985) *Biochim. Biophys. Acta 830*, 109−112.
Kim, P. S., & Baldwin, R. L. (1980) *Biochemistry 19*, 6124−6129.
Koradi, R., Billeter, M., & Wüthrich, K. (1996) *J. Mol. Graphics 14*, 51−55.
Laity, J. H., Shimotakahara, S., & Scheraga, H. A. (1993) *Proc. Natl. Acad. Sci. U.S.A. 90*, 615−619.
Li, L.-K., Riehm, J. P., & Scheraga, H. A. (1966) *Biochemistry 5*, 2043−2048.
Lin, L.-N., & Brandts, J. F. (1983) *Biochemistry 22*, 553−559.
Makhatadze, G. I., & Privalov, P. L. (1995) *Adv. Protein Chem. 47*, 307−425.
Marquardt, D. W. (1963) *J. Soc. Ind. Appl. Math. 11*, 431−441.
Montelione, G. T., Arnold, E., Meinwald, Y. C., Stimson, E. R., Denton, J. B., Huang, S.-G., Clardy, J., & Scheraga, H. A. (1984) *J. Am. Chem. Soc. 106*, 7946−7958.
Mui, P. W., Konishi, Y., & Scheraga, H. A. (1985) *Biochemistry 24*, 4481−4489.
Nozaki, Y. (1972) *Methods Enzymol. 26*, 43−50.
Oka, M., Montelione, G. T., & Scheraga, H. A. (1984) *J. Am. Chem. Soc. 106*, 7959−7969.
Pace, C. N., Shirley, B. A., & Thomson, J. A. (1989) in *Protein Structure: A Practical Approach* (Creighton, T. E., Ed.) pp 311−330, IRL Press, Oxford.
Pace, C. N., Vajdos, F., Fee, L., Grimsley, G., & Gray, T. (1995) *Protein Sci. 4*, 2411−2423.
Pincus, M. R., Gerewitz, F., Wako, H., & Scheraga, H. A. (1983) *J. Protein Chem. 2*, 131−146.
Press, W. H., Teukolsky, S. A., Vetterling, W. T., & Flannery, B. P. (1992) *Numerical Recipes in C*, 2nd ed., pp 451−455, Cambridge University Press, Oxford.
Privalov, P. L. (1979) *Adv. Protein Chem. 33*, 167−241.
Rehage, A., & Schmid, F. X. (1982) *Biochemistry 21*, 1499−1505.
Rothwarf, D. M., & Scheraga, H. A. (1993) *Biochemistry 32*, 2671−2679.
Santoro, J., González, C., Bruix, M., Neira, J. L., Nieto, J. L., Herranz, J., & Rico, M. (1993) *J. Mol. Biol. 229*, 722−734.
Santoro, M. M., & Bolen, D. W. (1988) *Biochemistry 27*, 8063−8068.
Scheraga, H. A. (1957) *Biochim. Biophys. Acta 23*, 196−197.
Scheraga, H. A. (1967) *Fed. Proc. 26*, 1380−1387.
Scheraga, H. A. (1984) *Carlsberg Res. Commun. 49*, 1−55.
Schmid, F. X. (1982) *Eur. J. Biochem. 128*, 77−80.
Schmid, F. X. (1983) *Biochemistry 22*, 4690−4696.
Schmid, F. X., & Baldwin, R. L. (1979) *J. Mol. Biol. 135*, 199−215.
Schmid, F., & Blaschek, H. (1984) *Biochemistry 23*, 2128−2133.
Schmid, F. X., Grafl, R., Wrba, A., & Beintema, J. J. (1986) *Proc. Natl. Acad. Sci. U.S.A. 83*, 872−876.
Schultz, D. A., Schmid, F. X., & Baldwin, R. L. (1992) *Protein Sci. 1*, 917−924.
Scott, R. A., & Scheraga, H. A. (1963) *J. Am. Chem. Soc. 85*, 3866−3873.
Sendak, R. A., Rothwarf, D. M., Wedemeyer, W. J., Houry, W. A., & Scheraga, H. A. (1996) *Biochemistry 35*, 12978−12992.
Stimson, E. R., Montelione, G. T., Meinwald, Y. C., Rudolph, R. K. E., & Scheraga, H. A. (1982) *Biochemistry 21*, 5252−5262.
Thannhauser, T. W., Konishi, Y., & Scheraga, H. A. (1987) *Methods Enzymol. 143*, 115−119.
Tsong, T. Y., Baldwin, R. L., & Elson, E. L. (1972) *Proc. Natl. Acad. Sci. U.S.A. 69*, 1809−1812.
Udgaonkar, J. B., & Baldwin, R. L. (1988) *Nature 335*, 694−699.
Udgaonkar, J. B., & Baldwin, R. L. (1990) *Proc. Natl. Acad. Sci. U.S.A. 87*, 8197−8201.
Udgaonkar, J. B., & Baldwin, R. L. (1995) *Biochemistry 34*, 4088−4096.
Wlodawer, A., & Sjölin, L. (1983) *Biochemistry 22*, 2720−2728.
Wlodawer, A., Miller, M., & Sjölin, L. (1983) *Proc. Natl. Acad. Sci. U.S.A. 80*, 3628−3631.
Wlodawer, A., Svensson, L. A., Sjölin, L., & Gilliland, G. L. (1988) *Biochemistry 27*, 2705−2717.
Woody, R. W., Friedman, M. E., & Scheraga, H. A. (1966) *Biochemistry 5*, 2034−2042.
Yao, M., & Bolen, D. W. (1995) *Biochemistry 34*, 3771−3781.

BI970711I